Chapter 3

Performance Improvement of ZnO CQDs/ TIPS-Pentacene Heterojunction based UV-Visible Photodetector using MoOx HTL

***Part of this work has been published as:**

Abhinav Pratap Singh and S. Jit, "Solution Processed ITO/ZnO QDs/TIPS - Pentacene/MoO_x High-Performance UV-Visible Photodetector," ***IEEE Photonics Technology Letters***, vol. 34, no. 19, pp. 1034–1037, **Oct. 2022**, DOI: 10.1109/LPT.2022.3199500.

Chapter 3

Performance Improvement of ZnO CQDs/ TIPS-Pentacene Heterojunction based UV-Visible Photodetector using MoOx HTL

3.1 Introduction

The performance improvement in the TIPS-pentacene (organic semiconductor) and ZnO CQDs based heterojunction UV photodetector has been discussed in Chapter-2. Moreover, it is found that the fabricated heterojunction UV photodetector has very high dark current due to high conductivity of ZnO layer. To overcome this drawback, the charge blocking layers can be used to provide photomultiplication phenomenon as observed from the literature review in Chapter-1. Motivated by this, we have introduced a thin MoOx layer (~10 nm) which is acting as electron blocking layer. In this chapter, we have proposed an ITO/ZnO CQDs/TIPS-P/MoOx/Ag based vertical photodetector structure where the MoOx layer is added to act as a hole transport layer. A vertical structure is adopted in our proposed organic-inorganic hybrid photodetector to improve its speed of transport layer (HTL). The proposed structure operates in both the UV and visible regions with enhanced performance operation as well as the stability of the TIPS-pentacene organic photoactive material of the device [14], [88]–[91]. The MoO_x based HTL prevents the electrons from reaching the anode side to minimize the electron-hole recombination, which, in turn, reduces the dark current and improves the overall performance parameters of the device [81][92]. The layer of colloidal ZnO CQDs (of average size ~ 2.00 nm) synthesized by the hot-injection route method [93]

[73] acts as the electron transport layer (ETL)-cum UV absorption region while the TIPS-Pentacene is used as the active material for UV and visible light absorption. The proposed photodetector works in the UV and visible regions at 386 nm and 640 nm, respectively.

In this chapter, experimental details regarding ZnO CQD synthesis and device fabrication steps has been outlined in section 3.2. Section 3.3 presents detailed absorption and Photoluminescence (PL) analysis of the ZnO, TIPS-Pentacene and MoOx layers followed by optoelectronic charecterization of the device, performance parameter extraction and comparison of obtained result with the recent reports. Finally the conclusion section 3.4 summarizes the key observations of the experiment and significance of electron blocking layer (EBL) in performance enhancement.

3.2 Experimental Details

3.2.1 Fabrication of Photodetector

The fabrication processing steps of the ITO/ZnO CQDs/ TIPS-Pentacene structure are similar to those described in our earlier work reported in [93]. The device diagram of the The ITO-coated glass substrates (15mm x 15mm) were first cleaned by ultrasonication method using a 1:6 ratio of soap solution and deionized (DI) water for 20 minutes. The substrates were then rinsed for 10 minutes in fresh DI water and then processed for plasma cleaning (Femto Science Inc. CUTE, Korea) in argon: oxygen (50:50 ratio). Zinc-acetate dihydrate, Ethylene glycol monomethyl ether or 2-methoxyethanol and monoethanolamine (MEA) chemicals (with 99.99% purity) procured from the Sigma-Aldrich were directly used for the synthesis of ZnO CQDs via the hot route injection approach described in prior works [93] [73]. The ZnO CQDs solution was spin-coated (using SPM-150LC TSE-system GmbH,

Germany) at 2000 rpm for 40 sec on the cleaned ITO coated glass substrates. The samples were then dried at 150° C for 5 minutes. This procedure was repeated 6 to 8 times to get a ~180 nm thickness (measured by F-20 Filmetrics, USA) of ZnO CQDs. The film was then heated at 450° C in an ambient environment using a hot plate. TIPS-Pentacene (Ossila Limited, U.K.) sol-gel prepared by dissolving it in the dichlorobenzene solution (10 mg/mL) was spin-coated at 1200 rpm for 50 sec followed by drying at 120° C for 1 h. Then a thin MoOx layer (~ 12 nm) was grown on the TIPS-Pentacene film by thermal evaporation unit (FL400 SMART COAT 3.0 A, Hind High Vacuum, India) at a 0.5 Å/sec deposition rate. Finally, pure silver (99.99 %) metal dots of 1 mm diameter (with 0.0314 cm^2 area) and 120 nm thickness were fabricated on the MoOx layer at a 0.2 Å /sec deposition rate under ~ 2.6×10^{-6} mbar chamber vacuum for anode contacts.

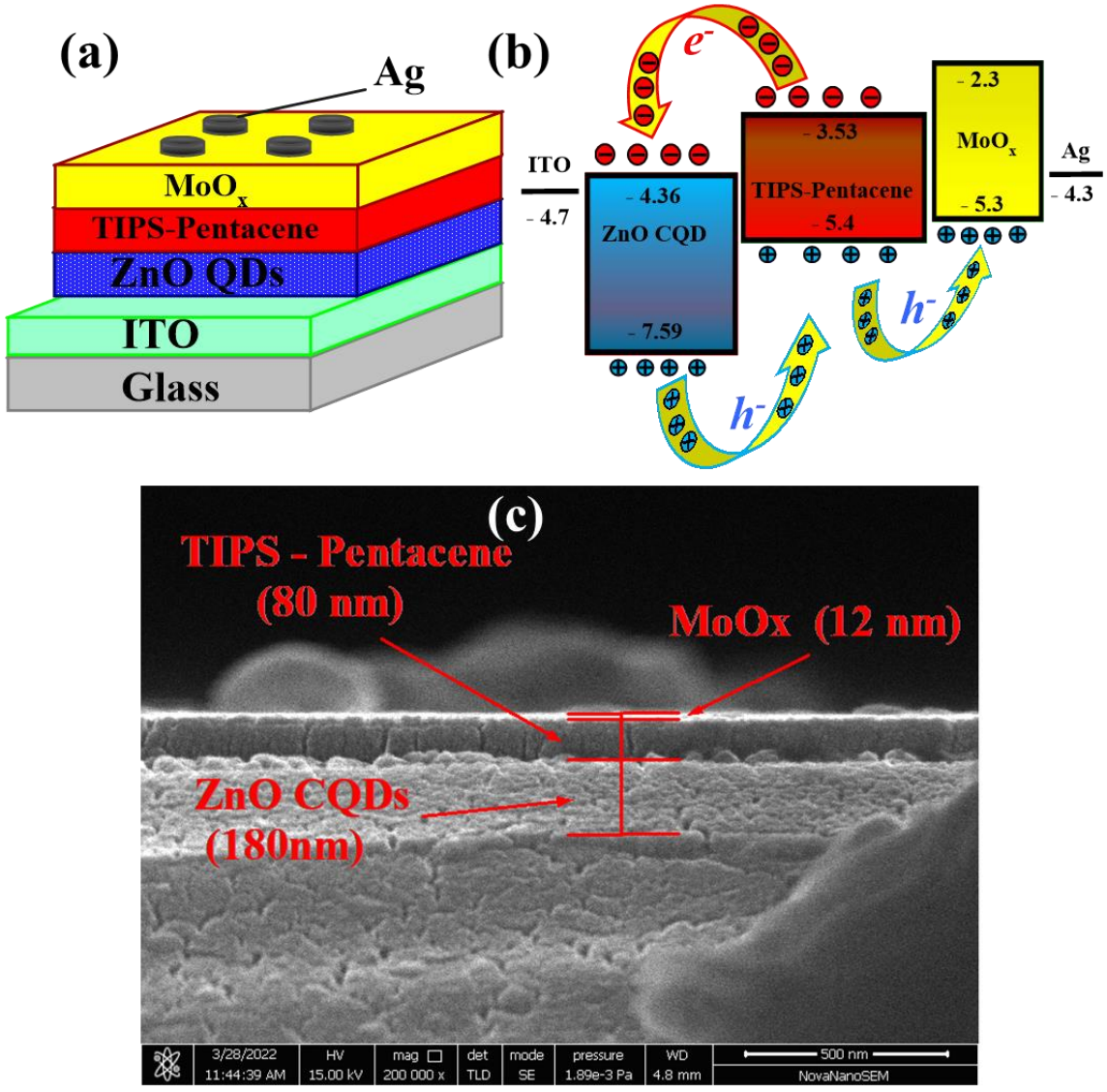

Figure 3.1 (a) Device diagram, (b) Band diagram (c) Crossectional FE-SEM of glass/ ZnO CQD/ TIPS-P/ MoO_x, the proposed device.

The proposed device structure and its energy band diagram are shown in Figure 3.1(a) and 3.1(b), respectively. The energy bandgap, in Figure 3.1(b). The fabricated device image used measurements is shown in Figure 3.1(c).

3.3 Results and Discussion

3.3.1. Structural and Optical Analysis of Thin Film

As discussed in Chapter 2, The Transmission Electron Microscopy (TEM) image (TECNAI G2 20 TWIN) of ZnO quantum dots The average particle size of ~ 2.0 nm was calculated from the histogram, which is smaller than its exciton Bohr's radius of 2.87nm [63]. This confirms the ZnO nanoparticles are QDs in nature. The continuous diffused concentric rings in the SAED confirm single crystalline ZnO QDs of high surface-to-volume ratio. The d-spacings of the ZnO QDs are obtained as 0.26 nm and 0.14 nm corresponding to <002> and <103> orientations, respectively, from the Crystallography Open Database (COD) number 2300112 [93].

3.3.2. Absorption and Photoluminescence (PL) Analysis

Figure 3.2 (a) compares the absorption spectra of ZnO CQDs, TIPS-P, MoO_x and the combination of ZnO CQD/ TIPS-P/ MoO_x obtain from the UV-Vis spectroscopic measurements (V-770 from JASCO, Japan). The absorption of ZnO CQDs/ TIPS-P/ MoO_x covers a wide range from UV to visible region due to the combined absorptions of ZnO CQDs and TIPS-P layers. Figure 3.2 (b) shows the photoluminescence (PL) of ZnO CQDs, TIPS-P, MoO_x and ZnO CQD/ TIPS-P/ MoO_x at the excitation wavelength (λ_{ex}) of 375 nm using the Edinberg's Spectrofluorometer FS980. No significant emissions are observed for MoO_x and TIPS-P in Figure 3.2 (b). The PL intensity of the ZnO CQDs (with peak at ~ 450 nm) is decreased with the increased wavelength in visible region. However, the PL of the ZnO CQD/ TIPS-P/ MoO_x combined structure (Figure 3.2 (b) (ii)) shows that the intensity of the TIPS-P is significantly increased in the visible region while the intensity level of the ZnO

CQDs is significantly reduced. This confirms the fast energy transfer from Zn CQD to TIPS-P due to adequate overlap between the emission of ZnO CQDs and absorption of TIPS-P films.

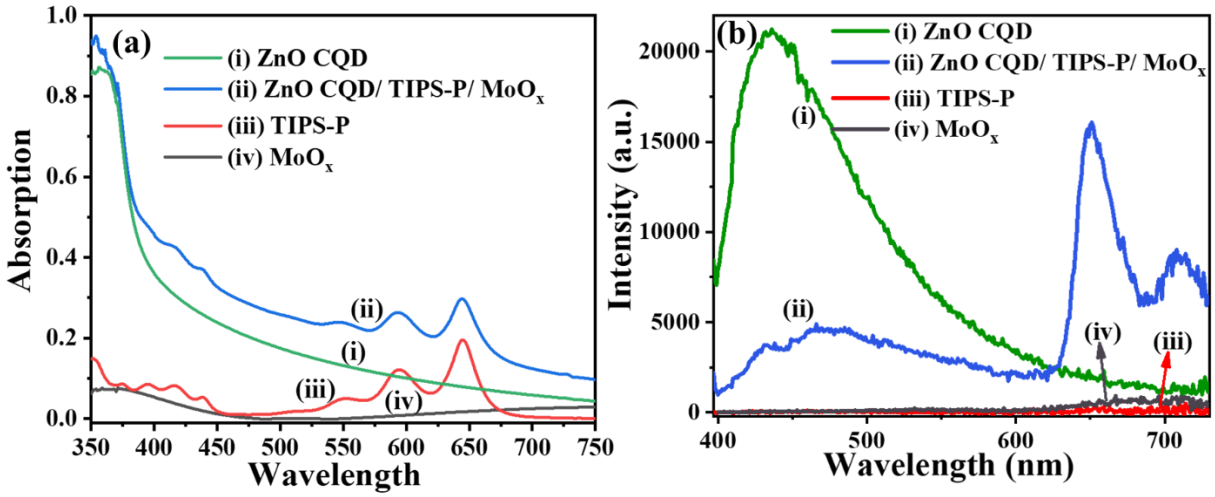

Figure 3.2 (a)Absorbance and (b) Emission of colloidal ZnO CQDs, TIPS-P MoO_x and ZnO CQDs/ TIPS -Pentacene /MoO_x.

3.3.3. Optoelectronic Characterization of Photodetector

The current-voltage (I-V) characteristics under illumination have been measured using the parameter analyzer (Keysight, USA), Xenon lamp and Monochromator (ATLAS 300, Camlin, U.K.). Figure 3.3 (a) compares the dark and photocurrents at 386 nm and 640 nm illumination. The measured dark current is 4.38×10^{-6} A while the maximum photocurrent is 8.4×10^{-4} A. The image of the fabricated device is shown in Figure 3.3 (b). The responsivity and detectivity characteristics measured over350-700 nm are shown in Figure 3.4. Under 1 V reverse bias, the maximum responsivity (R), detectivity (D^*) and external quantum efficiency (EQE) were estimated as 217.31 A/W, 6.79×10^{12} cmHz$^{1/2}$/W and ~ 69811%, respectively, at 386 nm, and incident optical power density of 64.8 μW/cm^2. For the Visible region, R ~57.34

A/W, D* ~ 1.79 × 10^{12} cmHz$^{1/2}$/W and EQE ~11111.3 % were obtained under incident illumination intensity of 48.8 µW/cm^2 at 640 nm and -1 V bias voltage and compared the results in table 3.1.

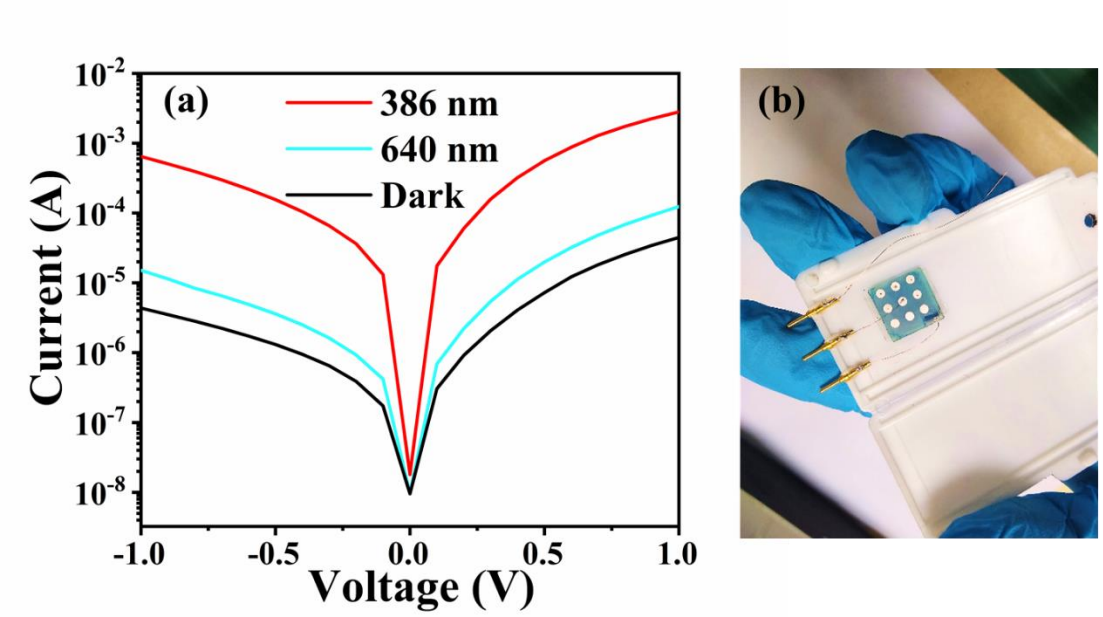

Figure 3.3 (a) I-V characteristic of the proposed device (b) Fabricated device image.

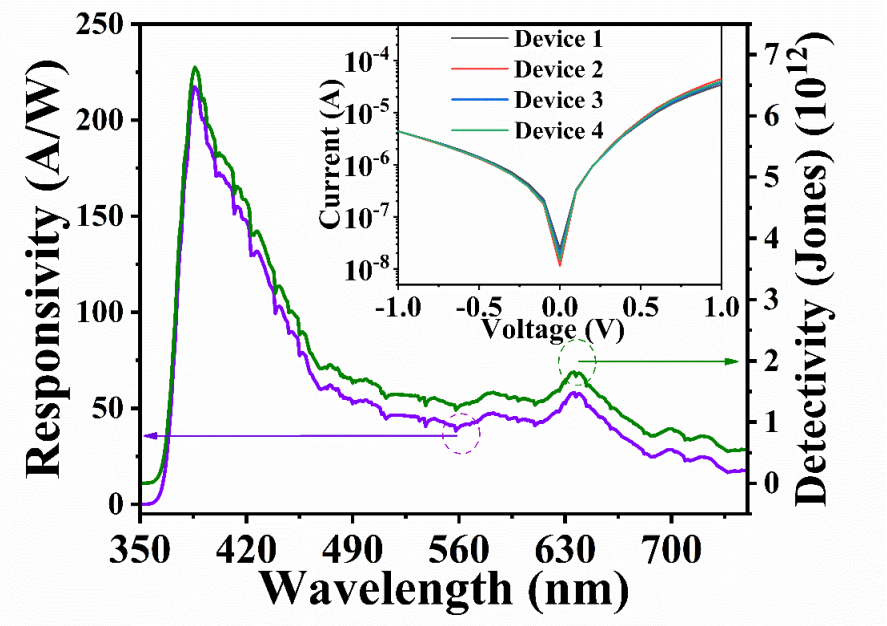

Figure 3.4 Responsivity, Detectivity characteristic of device ITO/ZnO CQDs/TIPS-P/ MoO_x/Ag and inset graph shows the reproducibility of four different devices

TABLE 3.1 COMPARISON OF RESPONSIVITY AND DETECTIVITY OF ZNO BASED PHOTODETECTORS

Device Structure	Applied Voltage	Power density (W/cm2)	Spectral range (nm)	Responsivity (AW-1)	Detectivity (Jones)	EQE	Ref.
ITO / ZnO NR /P3HT / Au NPs / PEDOT:PSS /Ag	-2 V	3m	370	17.7	-	-	[27]
ITO / Cu2O / PVK / ZnO NR / Ag	-1 V	24.9u	360	13.28	1.03×10^{13}	-	[29]
ITO / ZnO NR / P3HT / PEDOT:PSS / Ag	-2 V	3m	370	10.7	-	-	[27]
ITO / TiO2 / P3HT:PCBM /Al	-1 V	60m	550 370	0.5 0.2	1.9×10^{12}	113	[30]
ITO/interlayer / P3HT:ITIC / MoOx / Al	-20 V	-	360	-	2.15×10^{12}	19300	[29]
ITO / PEDOT:PSS/ P3HT:PTB7-TH:PC71BM / Al	-25 V	-	390 625 750	284.9 423.4 5.2	-	90700 84100 850	[23]
ITO / PEDOT:PSS/F8T2:ZnO NPs / BCP / Al	-15 V	-	360 510	6.39 0.89	-	2170 220	[30]
ITO / ZnO / PEDOT:PSS /Au	-1 V	8m (UV) 2m (Blue) 7m (Green) 2m (Orange)	UV Blue Green Orang	0.013 0.005 0.002 0.001	-	-	[85]
ITO/ZNO CQDs/TIPS-Pentacene/ Ag	-1V	43 u	375	59.15	7.01×10^{13}	19877	Previous work [93]
ITO/ZNO CQDs/ TIPS-Pentacene / MoOx / Ag	-1 V	6.48×10^{-5} 4.88×10^{-5}	386 640	217.31 57.34	6.79×10^{12} 1.79×10^{12}	69811.9 11111.3	This Work

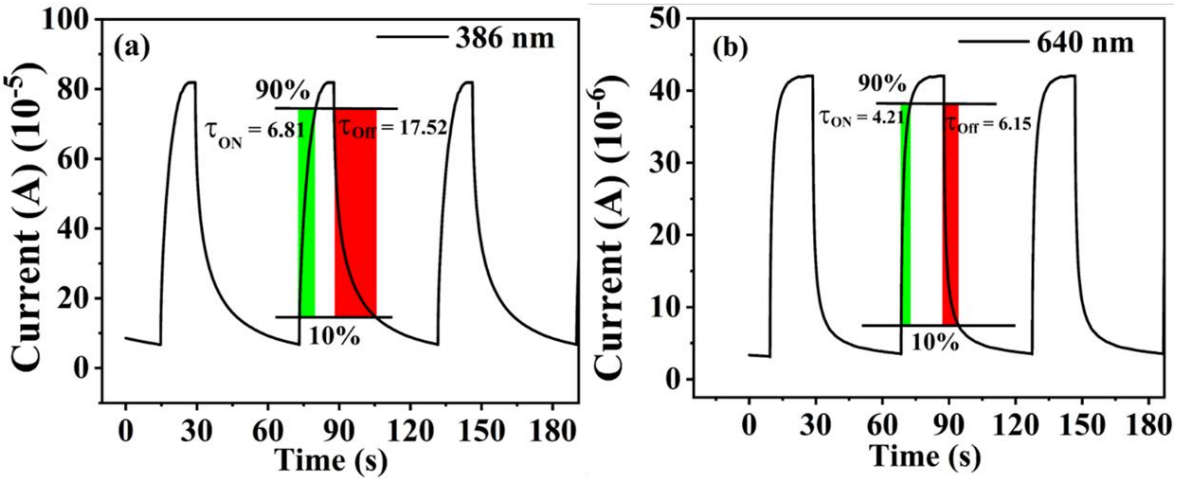

Figure 3.5 Transient response of the device (a) at 386 nm wavelength and (b) at 640 nm wavelength.

The EQE above 100% is attributed to the photomultiplication phenomenon in the organic-organic photodetectors. Under reverse bias operation, a part of the photogenerated electrons gets trapped in the ZnO CQDs while the rest is collected by the ITO cathode. The accumulation of these trapped electrons results in photo multiplication to enhance the EQE of the device beyond 100% [81][23]. The transient response characteristics shown in Figure 3.5 give the respective values of rise time and fall time of 6.81 s and 17.52 s at 386 nm (power density of 64.8 μW/cm^2); and 4.21 s and 6.15 s at 640 nm (power density of 48.8 μW/cm^2) for an incident optical pulse with equal ON and OFF of 60 s. The response times appear to be a bit high possibly due to the defects in ZnO CQDs/TIPS-P interface, high RC constant [86] [87] and traps in ZnO CQDs film resulted from all the fabrication and characterization processes carried out in an open ambient without using any clean room facility and controlled environmental conditions. Finally, the stability of the proposed photodetector is investigated in Figure 3.6. The degradation of the responsivity and detectivity are studied over a period of nearly 15 weeks. A small degradation is observed due to open ambient measurements of the

unpackaged device under study. It is believed that the device performance can be improved by fabricating the device in an controlled environment followed by its proper packaging.

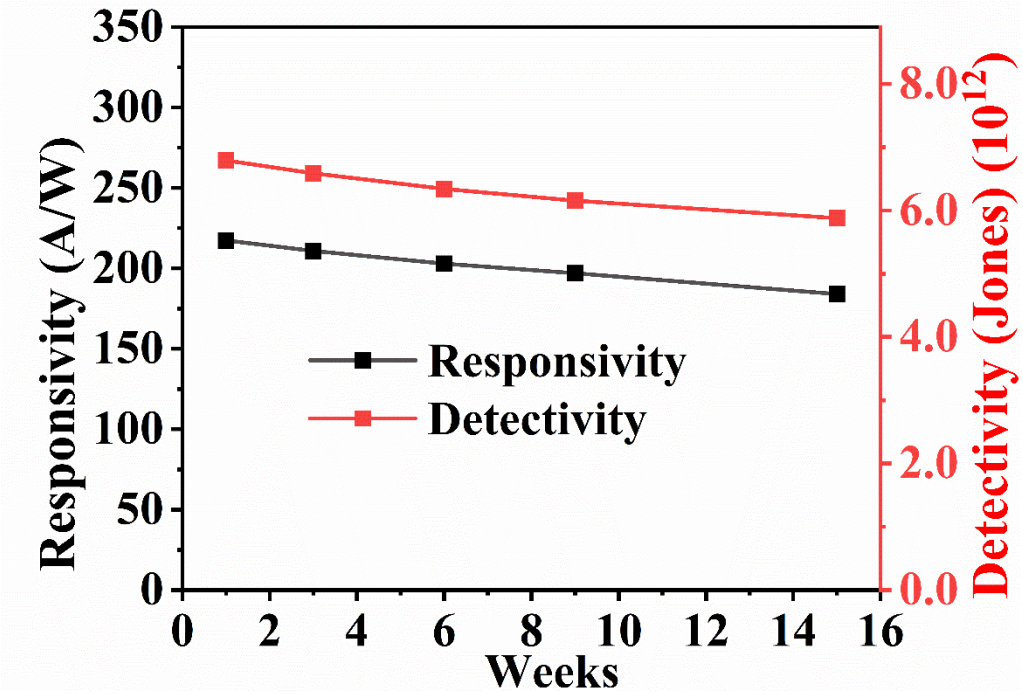

Figure 3.6 Stability results of the proposed device for of 15 weeks in terms of responsivity and detectivity.

3.4 Conclusion

The main goal of work reported in this chapter was to enhance overall performance of the device including drawback of Chapter 2. In this particular chapter the device performance has been enhanced by using hole transport layer (HTL) engineering. The effect of MoOx HTL layer is investigated with ZnO CQDs/TIPS-P hetrostructure structure. The MoOx layer acts as the HTL to improve the performance by reducing the recombination current in the device as well as acting as electron blocking layer to suppress the dark current. The device is found to exhibit a maximum responsivity of 217.31 A/W, EQE of ~ 69811% and detectivity

of ~ 6.79 × 10^{12} cmHz$^{1/2}$/W under the light intensity of ~ 64.8 μW/cm^2 at 386 nm, in the UV region and a maximum responsivity of ~57.34 A/W, EQE of ~11111.3 % and detectivity of ~ 1.79 × 10^{12} cmHz$^{1/2}$/W under the light intensity of 48.8 μW/cm^2 in the visible region at 640 nm, operated at a bias voltage of -1 V.